



pubs.acs.org/journal/estlcu Letter

Impact of Sampling Type, Frequency, and Scale of the Collection System on SARS-CoV-2 Quantification Fidelity

Andrea D. George, Devrim Kaya, Blythe A. Layton, Kestrel Bailey, Scott Mansell, Christine Kelly, Kenneth J. Williamson, and Tyler S. Radniecki*



Cite This: Environ. Sci. Technol. Lett. 2022, 9, 160-165



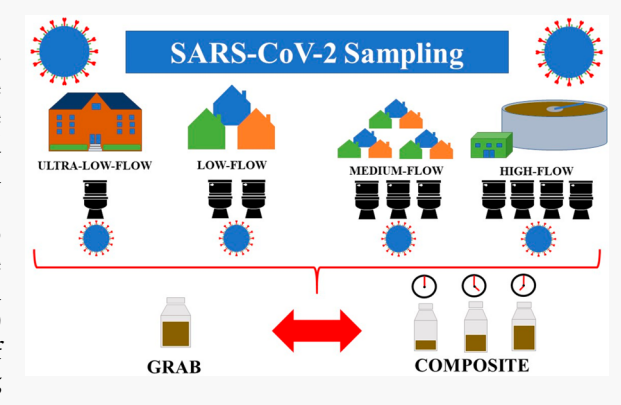
ACCESS

III Metrics & More

Article Recommendations

s) Supporting Information

ABSTRACT: With the rapid onset of the COVID-19 pandemic, wastewater-based epidemiology sampling methodologies for SARS-CoV-2 were often implemented quickly and may not have considered the unique drainage catchment characteristics. This study assessed the impact of grab versus composite sampling on the detection and quantification of SARS-CoV-2 in four different catchment scales with flow rates ranging from high flow (wastewater treatment plant influent) to medium flow (neighborhood scale) to low-flow (city block scale) to ultralow flow (building scale). At the high-flow site, grab samples were comparable to 24 h composite samples with SARS-CoV-2 detected in all samples and differed in concentration from the composite by <1 log 10 unit. However, as the size of the catchment decreased, the percentage of negative grab samples increased despite all respective composites being positive, and the SARS-CoV-2 concentrations of grab samples varied



from those of the composites by up to almost 2 log 10 units. At the ultra-low-flow site, increased sampling frequencies generated composite samples with higher fidelity to the 5 min composite, which is the closest estimate of the true SARS-CoV-2 composite concentration that could be measured. Thus, composite sampling is more likely to compensate for temporal signal variability while grab samples do not, especially as the catchment basin size decreases.

INTRODUCTION

Grab sampling and composite sampling are the two most commonly used sampling approaches in wastewater-based epidemiology (WBE) for SARS-CoV-2. Composite sampling has been used to improve detection given the uncertainty of shedding rates, temporally variable pulse inputs, and fluctuations in diurnal wastewater flow rate. A downside to composite sampling is that it requires investing in costly and cumbersome equipment (e.g., autosamplers). Thus, grab sampling has also been used to monitor SARS-CoV-2 in wastewater treatment plant (WWTP) influents and low-flow sewers leaving buildings.

While it is cheaper, faster, and less laborious than composite sampling, there are concerns surrounding the accuracy of grab sampling due to the discrete and variable nature of SARS-CoV-2 inputs into a catchment. Likewise, the 1 h sampling frequency for creating 24 h composites is frequently used for monitoring large catchment basins where there is significant time and flow for the dispersion of a target signal. However, it is unclear if this sampling frequency is adequate to accurately capture SARS-CoV-2 signals at much lower flow rates closer to the input source, where time and flow for dispersion are minimal. An inadequate sampling approach may introduce unintended biases, including false negatives and gross over- or

underestimation of average daily viral concentrations due to missing or capturing the tails or peak of the temporally variable pulse input.

This study identifies the impact of sampling type and frequency on SARS-CoV-2 detection and quantification in wastewater samples collected from several catchment scales, ranging from influent at a WWTP to a cluster of buildings on a college campus. This study also provides insight into the temporal variability of SARS-CoV-2 concentrations under various flow regimes and how that may impact the interpretation of results generated by the grab versus composite sampling approaches.

■ MATERIALS AND METHODS

Sampling Process and Site Description. Three sites with low, medium, and high flow rates in Forest Grove, OR, were selected for 24 h sampling. The low-flow site (0.42 m³/

Received: November 1, 2021 Revised: January 10, 2022 Accepted: January 11, 2022 Published: January 18, 2022





Table 1. Summary of Results at Different Flow Scales and Sampling Frequencies^a

site	no. of grab samples (n)	total sampling time (h)	average dry weather flow rate (GPM)	sampling frequency	composite concentration (log ₁₀ gc/L)	maximum grab concentration (log ₁₀ gc/L)	minimum grab concentration (log ₁₀ gc/L)	percent non- detects (%)	percent grabs below composite (%)	MAE	RMSLE
ultra-low- flow	32	8	13 ^c	15 min	5.81 ± 0.08^b	7.16 ± 0.02	3.44 ± 0.04	40.6	93.8	1.87	1.95
low-flow	21	24	111	1 h	4.77 ± 0.03	5.54 ± 0.01	3.69 ± 0.05	38.1	76.2	1.00	0.78
medium- flow	24	24	700	1 h	3.92 ± 0.10	4.66 ± 0.02	3.57 ± 0.05	37.5	70.8	0.29	0.32
high-flow	24	24	2430	1 h	3.95 ± 0.13	4.47 ± 0.04	3.48 ± 0.06	0.0	58.3	0.24	0.29
Hours 1–2											
ultra-low- flow	24	2	13 ^c	5 min	5.88 ± 0.09^{b}	7.16 ± 0.02	3.57 ± 0.05	25.0	91.7	1.67	1.77
ultra-low- flow	12	2	13 ^c	10 min	6.17 ± 0.15^b	7.16 ± 0.02	3.57 ± 0.05	16.7	91.7	1.90	2.03
ultra-low- flow	8	2	13 ^c	15 min	6.31 ± 0.20^{b}	7.16 ± 0.02	3.57 ± 0.05	12.5	87.5	2.06	2.14
Hours 1–8											
ultra-low- flow ^d	32	8	13 ^c	15 min	5.81 ± 0.08^b	7.16 ± 0.02	3.44 ± 0.04	40.6	93.8	1.87	1.95
ultra-low- flow	16	8	13 ^c	30 min	6.03 ± 0.12^b	7.16 ± 0.02	3.57 ± 0.05	43.8	93.8	2.00	2.11
ultra-low- flow	9	8	13 ^c	1 h	6.28 ± 0.21^b	7.16 ± 0.02	3.57 ± 0.05	33.3	88.9	1.95	2.13

^aThe low-flow site had 3 h that were not analyzed (one due to no sample collection and two due to RNA extraction failures). Ultra-low-flow composite concentrations (*) were calculated *in silico* from the corresponding grab samples. Ultra-low-flow 15 min results (***) are shown twice for the purpose of comparison. MAE = mean absolute error. RMSLE = root-mean-square log error. ^bThese composites were created digitally using the respective grab samples. ^cThis flow was estimated using the number of residents and a 67 GPD/resident flow estimate based on previous wastewater data in the region. ^dThis series is shown twice for the purpose of comparison.

min average dry weather flow) serves 400 people in a small residential community while also receiving industrial discharge from three food processing plants with 24 h operations. The medium-flow site (2.65 m³/min average dry weather flow) receives most of its flow from a 2200-person residential community with some small commercial businesses. The highflow site (9.20 m³/min average dry weather flow) is the influent to the Forest Grove WWTP that serves approximately 48000 residents and receives a mixture of industrial wastewater. Infection rates ranged from 11 to 34 cases per 10000 people at the time of sampling, with an approximate infection rate of 11 cases per 10000 people at the low-flow site, 23 cases per 10000 people at the medium-flow site, and 34 cases per 10000 people at the high-flow site (case data from the Oregon Health Authority, https://public.tableau.com/app/profile/ oregon.health.authority.covid.19/viz/OregonCOVID-19 Casesby ZIP Code-Summary Table/ CasesbyZIPCodeSummaryTable).

Hourly grab samples (200 mL) were taken from the low-medium-, and high-flow sites with an ice-cooled 24-bottle ISCO 3700 autosampler (Teledyne ISCO, Lincoln, NE) over a 24 h period, designed to capture peak solid concentrations (shown by TSS/COD values in Table S1). Time-weighted composite samples were prepared by combining 10 mL of each hourly grab sample together.

An additional site with ultralow flow was selected from a separate, neighboring sewershed serving four college dormitory buildings, one of which was used to temporarily house COVID-19-infected students for convalescence. This site had three known cases per 279 people (108 cases per 10000 people) and an estimated flow rate of 0.05 m³/min. Grab samples (400 mL) were collected every 15 min for an 8 h period (designed to capture peak solid concentrations) and every 5 min in the first 2 h. Every 2 h, the autosampler was

removed and bottles were replaced; these transitions caused four grab samples to be missed (11:15, 13:30, 15:45, and 16:00). Time-weighted composites were calculated *in silico* by averaging the SARS-CoV-2 concentrations of the respective grab samples.

Sample Concentration. Samples were stored at -20 °C for 1-50 days before concentration (Table S1). A 57 day freezer decay experiment showed minimal decay in the SARS-CoV-2 RNA signal $[k = 0.0121 \text{ day}^{-1} \text{ (Figure S1)}]$, and thus, the uncorrected data are presented here; decay-corrected sample data are listed in Table S2. Frozen samples were thawed in a warm water bath (~30 °C) and concentrated by filtering samples (10-50 mL) through an electronegative mixed cellulose ester membrane filter (catalog no. 7141-104, Whatman, Buckinghamshire, U.K.). Following filtration, filters were placed in 2 mL tubes containing 0.7 mm garnet beads and 1 mL of DNA/RNA Shield (Zymo Research, Irvine, CA) and stored at -80 °C for 1-17 days (mean of 6 ± 4 days) until RNA extraction. Concentration method recovery was estimated to be 57% using a surrogate spike [bovine coronavirus (see the Supporting Information)].

RNA Extraction. Filters stored in DNA/RNA Shield were thawed at room temperature (~20 °C) and homogenized using a BioSpec Mini-Beadbeater 16 (BioSpec Products, Inc., Bartlesville, OK) for 2 min. After cooling on ice for 2 min, the samples were centrifuged at 12000 rcf for 1 min. Approximately 700 μ L of lysate was transferred from each tube to a 96-well plate. RNA was extracted from 200 μ L of lysate using the MagMAX Viral/Pathogen kit on a KingFisher automated instrument (ThermoFisher Scientific, Waltham, MA). Purified RNA was eluted in 50 μ L of elution buffer provided with the kit. Positive SARS-CoV-2 RNA controls containing the N gene and human RNase P and negative controls containing human RNase P RNA (Exact Diagnostics, Fort Worth, TX) were

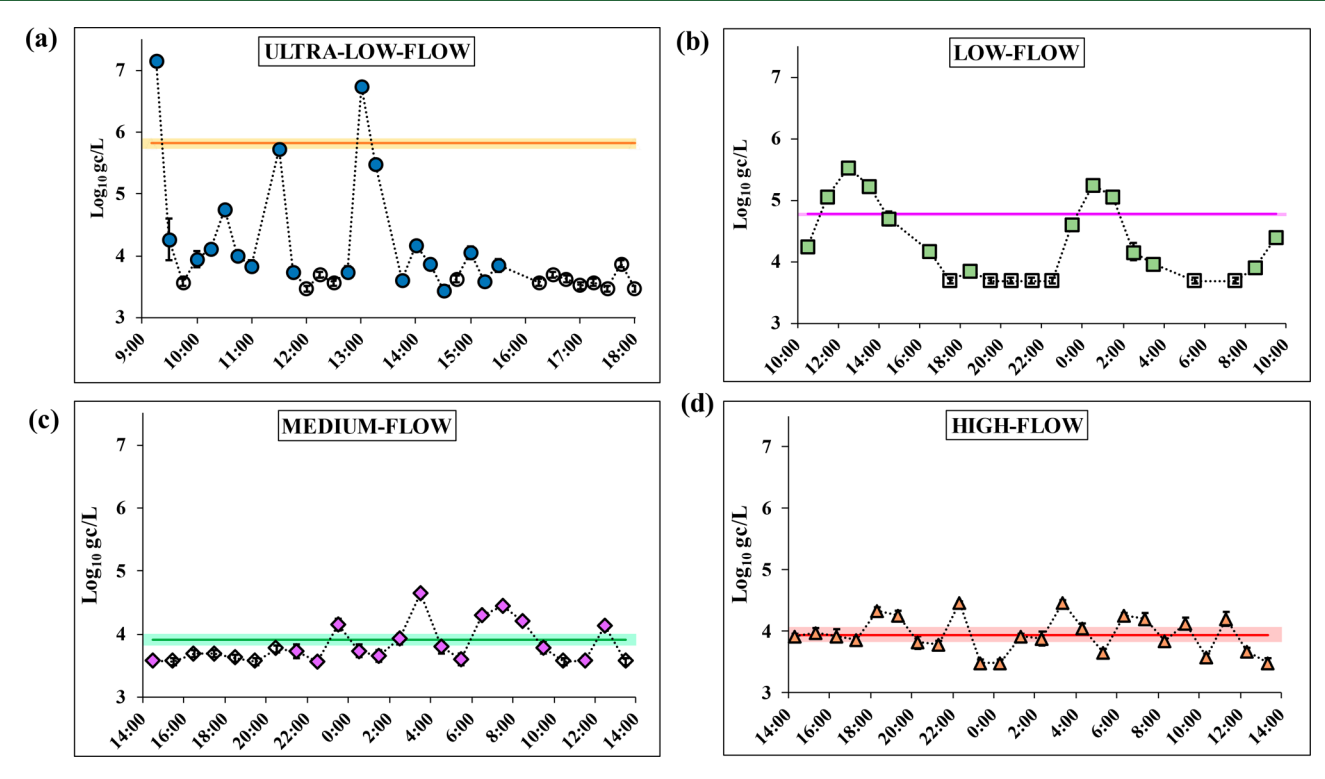


Figure 1. SARS-CoV-2 concentrations over time from grab samples collected from (a) ultra-low-flow (15 min sampling frequency), (b) low-flow, (c) medium-flow, and (d) high-flow sites. The solid line denotes the composite value for each time series. The error bars on the grab samples and the shaded range on the composite lines denote standard errors. Non-detects are represented by empty symbols.

included in each extraction batch. Extraction blanks (phosphate-buffered saline) were also included with every batch. Reverse transcriptase droplet digital PCR (RT-ddPCR) immediately followed RNA extraction and purification.

Reverse Transcriptase Digital Droplet PCR. SARS-CoV-2 RNA was quantified using a commercial triplex assay (2019-nCoV CDC ddPCR Triplex Probe Assay, Bio-Rad catalog no. 12008202) and the One-Step RT-ddPCR Advanced Kit for Probes on the QX-200 ddPCR system (Bio-Rad, Hercules, CA). This assay uses the CDC's N1 and N2 primers with RNase P included as an internal control; the primer and probe sequences (Table S3) were published previously.7 An automated droplet generator produced an average of 12283 (±2227) droplets per reaction. Duplicate analyses were performed for each sample and control. Notemplate controls were included on each plate. The one-step thermal cycling conditions were as follows: reverse transcription at 50 °C for 60 min, enzyme activation at 95 °C for 10 min, 40 cycles of denaturation at 94 °C for 30 s followed by annealing/extension at 55 °C for 60 s, enzyme inactivation at 98 °C for 10 min, and finally a 4 °C hold for droplet stabilization, for a minimum of 30 min to a maximum of overnight. Finally, the amplification in the droplets was determined using the Bio-Rad droplet reader. The number of gene copies per partition was on average 0.00873 ± 0.0506 [standard deviation (SD)]. All assay conditions were performed as specified in the Bio-Rad assay protocol.8

Data Analysis. The QuantaSoft Analysis Pro software (version 1.0.596, Bio-Rad) was used to manually call droplet clusters for each target. R (version 4.0.2) with Rstudio Desktop (version 1.3.1056) and Microsoft Excel were used for all other analyses and graphics. N1 and N2 concentrations showed

good agreement, and thus, their geometric mean was used for all analyses (Figure S2).

Two different error metrics were employed to determine the impact of sampling approaches on SARS-CoV-2 quantification at different drainage basin scales. The first, mean absolute error (MAE), quantifies the average discrepancy between the SARS-CoV-2 concentrations observed in the grab samples versus the composite sample at each site (eq S1). The second, root-mean-square log error (RMSLE), applies more weight to outliers than the MAE, while also penalizing grab samples with concentrations below the composite value more than those above it (eq S2). ^{10,11} The results of the calculations used to compare the scales of flow are listed in Table 1 (eqs S1–S4).

The error associated with different scales of sampling frequency was explored using the time series from the ultra-low-flow site. For error metric analyses over the first 2 h, the 5 min composite SARS-CoV-2 concentrations were compared to concentrations at three grab sampling frequencies [5, 10, and 15 min (Figure S3)]. The 5 min frequency composite was as close to continuous sampling as could be reasonably obtained and therefore provides the best estimate of the true SARS-CoV-2 composite concentration during that time. Likewise, for error metric analyses over the entire 8 h, the 15 min composite SARS-CoV-2 concentrations were compared to the grab sample concentrations at 15, 30, and 60 min sampling frequencies (Figure S4).

Quality Control. Samples were accepted for data analysis only if the corresponding extraction blank, field blank, negative control, and no-template control (NTC) were all non-detects. Reactions with fewer than 6000 droplets were excluded (n = 4). Samples were excluded if the RNase P internal control failed [i.e., the sample was non-detect for all three targets (n = 2)]. A threshold of three positive droplets was used to define a

positive reaction. All targets were amplified in the positive controls. Extraction blanks, no-template controls, and negative controls were all non-detect. The limit of detection (LOD) was determined empirically to be 8 copies per reaction for N1 and 12 copies per reaction for N2 (see the Supporting Information). The SARS-CoV-2 concentration of the sample was aggregated with a geometric mean (eq S5). Non-detect values were replaced with half of the sample-specific LOD when calculating the mean (Table S4). Each sample-specific LOD shown in Table S4 was calculated from the empirical LOD (gc/reaction) for N1 and N2 and aggregated with a geometric mean (eqs S5 and S6). Data were analyzed without correction for method recovery and without normalization to a fecal indicator. The dMIQE checklist can be found in Table S5, with supporting data in Figures S5 and S6.

■ RESULTS AND DISCUSSION

Effect of Sampling Type on the Detection of the Presence or Absence of SARS-CoV-2. One application of WBE is to use the presence or absence of the SARS-CoV-2 signal in a wastewater sample to monitor the presence of COVID-19 in the community. At all four flow scales, SARS-CoV-2 was detected in the composite samples at concentrations above the sample-specific LOD. Additionally, all grab samples at the high-flow site (i.e., WWTP) yielded SARS-CoV-2 concentrations greater than the sample-specific LOD, similar to that of a recent study comparing composites collected over 1 and 24 h at a WWTP. However, as the wastewater flow decreased, the occurrence of non-detects in grab samples increased from 0% at the high-flow sites to 38.1% at the low-flow sites and to 40.6% at ultra-low-flow locations (Table 1).

The increased frequency of non-detects in grab samples at lower-flow sites located closer to the input source suggests that the SARS-CoV-2 signal did not have enough time to spread out via dispersion mechanisms. This was also reflected in the difference between the maximum and minimum SARS-CoV-2 concentrations observed at each location. This value was highest at the ultra-low-flow site (3.72 log_{10} gc/L) and decreased consistently as the flow increased, down to 0.47 log₁₀ gc/L at the high-flow site (Figure 1). These results indicate grab samples may be acceptable at high-flow sites (e.g., WWTP influent) for analyses of the presence or absence, although this may change if the SARS-CoV-2 prevalence is low in the community.^{2,13} However, at low-flow or ultra-low-flow sites (e.g., individual buildings), where SARS-CoV-2 signals appear in short bursts, composite sampling provides the most reliable information regarding the presence of a signal.

Effect of Sampling Type on Quantification of SARS-CoV-2. The largest relative error between the grab samples and their respective composites was observed at the ultra-low-flow site with MAE and RMSLE values of 1.87 and 1.95, respectively (Table 1). As the size of the catchment increased, the difference between the SARS-CoV-2 concentrations of the grab and composite samples decreased, with the high-flow site having MAE and RMSLE values of 0.24 and 0.29, respectively. Thus, as the scale of the flow increased, the relative error decreased and the grab samples became more representative of the composite value (Figure S7).

A recent study found that more than half of grab samples collected every 2 h from a WWTP influent were within 50% of their respective 24 h flow-weighted composite SARS-CoV-2 concentrations.¹⁴ In the study presented here, 46% of the samples were found to be within 50% of the time-weighted

composite at the high-flow site. Additionally, the grab sample SARS-CoV-2 concentrations at the high-flow site were fairly well-distributed around the composite sample concentrations, with just more than half (58.3%) of the grab sample values falling below the composite sample values.

In contrast, at the lower-flow sites grab sample SARS-CoV-2 concentrations differed from their time-weighted composite sample values by almost ≤2 orders of magnitude. Additionally, the distribution of the grab sample values around the composite sample concentrations was no longer symmetrical (Figure 1). At the low-flow and ultra-low-flow sites, 76−94% of the grab sample concentrations were below the composite sample SARS-CoV-2 concentration (Table 1). Times of peak solid concentration did not correspond with grab samples with the smallest error (compared to the composite) or the highest SARS-CoV-2 concentration at the site.

These results indicate that while grab samples may be fairly representative of the SARS-CoV-2 composite concentrations at high-flow sites (e.g., a WWTP influent), they fail to provide representative SARS-CoV-2 composite concentrations at lower-flow sites (e.g., buildings), which may lead to over- or underestimates of daily viral burden. The high variability at lower-flow sites closer to the input source is indicative of limited SARS-CoV-2 dispersion by that point in the conveyance system and highlights the need for composite sampling at such locations.

Effect of Sampling Frequency on Quantification of SARS-CoV-2. Time-weighted 24 h wastewater composites are frequently created by collecting samples hourly. Recent studies have used higher sampling frequencies, ranging from 10 to 30 min, to monitor building-scale catchments. ^{12,15} Given the high variability of SARS-CoV-2 concentrations at the ultra-low-flow site (Figure 1a), the sampling frequency was increased every 5 min for the first 2 h (Figure S3a) followed by a 15 min sampling frequency for the following 6 h of collection (Figure 1a).

For the 2 h sampling period, the MAE and RMSLE increased with a decrease in sampling frequency, with the highest values obtained from 15 min sampling (Table 1). This was also observed in the 8 h sampling period, except for the 1 h frequency MAE where there was an error that was slightly smaller than that of the 30 min frequency (this was not observed in the RMSLE, however). This demonstrates that a reduced sampling frequency can result in the composite sample capturing less of the temporal variation of SARS-CoV-2 concentrations and reduces the accuracy of the composite sample's SARS-CoV-2 concentration. Thus, at ultra-low-flow sites, it is advisable to increase the sampling frequencies to the greatest extent possible.

Recommendations for Sampling Plan Design. Multiple factors should be considered in selecting the site-specific sampling method to ensure the integrity of the data. Among those factors, the scale of the catchment appears to strongly influence the results and, thus, the sampling plan design by increasing the need for composite sampling at lower scales of flow. Additionally, the sampling frequency should also be considered, with special efforts to increase the frequency at the individual building/campus level. Neither of these factors exists outside monetary and equipment restrictions; therefore, consideration should be given to the type of information desired to be obtained from the sampling (e.g., presence or absence vs quantitative) for better utilization and interpretation of the results. Because this study sampled sewersheds in

different time periods with varying infection rates, future work may benefit from following SARS-CoV-2 RNA emitted during the same period throughout the sewershed and at different basin scales. It also may be beneficial to explore how unique site characteristics such as local industry, population density (e.g., neighborhood, college campus, etc.), or geographical variation may influence the detection and quantification of SARS-CoV-2 RNA and, thus, the sampling plan design.

ASSOCIATED CONTENT

Supporting Information

The Supporting Information is available free of charge at https://pubs.acs.org/doi/10.1021/acs.estlett.1c00882.

Results of the freezer decay experiment (Figure S1), N1 versus N2 for all samples (Figure S2), comparison of composites generated from 5 min grab samples using three sampling frequencies (Figure S3), comparison of composites generated from 15 min grab samples using three sampling frequencies (Figure S4), typical fluorescence plots for ddPCR (Figure S5), intraexperiment repeatability (Figure S6), box plots showing the decreasing error range with an increasing catchment size (Figure S7), storage time, volume concentrated, and fecal loading for each sample (Table S1), decay-corrected sample data (Table S2), primer and probe sequences used (Table S3), and dMIQE checklist (Table S4) (PDF)

AUTHOR INFORMATION

Corresponding Author

Tyler S. Radniecki — School of Chemical, Biological, and Environmental Engineering, Oregon State University, Corvallis, Oregon 97331, United States; orcid.org/0000-0002-5295-3562; Email: tyler.radniecki@oregonstate.edu

Authors

Andrea D. George – Department of Research & Innovation, Clean Water Services, Hillsboro, Oregon 97123, United States; School of Chemical, Biological, and Environmental Engineering, Oregon State University, Corvallis, Oregon 97331, United States

Devrim Kaya – School of Chemical, Biological, and Environmental Engineering, Oregon State University, Corvallis, Oregon 97331, United States

Blythe A. Layton – Department of Research & Innovation, Clean Water Services, Hillsboro, Oregon 97123, United States

Kestrel Bailey – Department of Research & Innovation, Clean Water Services, Hillsboro, Oregon 97123, United States

Scott Mansell – Department of Research & Innovation, Clean Water Services, Hillsboro, Oregon 97123, United States

Christine Kelly – School of Chemical, Biological, and Environmental Engineering, Oregon State University, Corvallis, Oregon 97331, United States

Kenneth J. Williamson – Department of Research & Innovation, Clean Water Services, Hillsboro, Oregon 97123, United States

Complete contact information is available at: https://pubs.acs.org/10.1021/acs.estlett.1c00882

Notes

The authors declare no competing financial interest.

Preprint version of this work: George, A. D.; Kaya, D.; Layton, B. A.; Bailey, K.; Kelly, C.; Williamson, K. J.; Radniecki, T. S. The Impact of Sampling Type, Frequency and Scale of Collection System on SARS-CoV-2 Quantification Fidelity. *medRxiv* https://doi.org/10.1101/2021.07.07.21260158 (accessed 2022-01-07).

ACKNOWLEDGMENTS

This work was supported by National Science Foundation RAPID Grant 2027679. Clean Water Services participated in this research with partial funding from the CARES Act through the Washington County Cities and Special District Assistance program. The authors acknowledge the assistance with sampling from Jason Cook and Jacob DeMartino of Clean Water Services.

■ REFERENCES

- (1) Ahmed, W.; Angel, N.; Edson, J.; Bibby, K.; Bivins, A.; O'Brien, J. W.; Choi, P. M.; Kitajima, M.; Simpson, S. L.; Li, J.; Tscharke, B.; Verhagen, R.; Smith, W. J. M.; Zaugg, J.; Dierens, L.; Hugenholtz, P.; Thomas, K. V.; Mueller, J. F. First Confirmed Detection of SARS-CoV-2 in Untreated Wastewater in Australia: A Proof of Concept for the Wastewater Surveillance of COVID-19 in the Community. *Sci. Total Environ.* **2020**, 728, 138764.
- (2) Ahmed, W.; Bivins, A.; Bertsch, P. M.; Bibby, K.; Gyawali, P.; Sherchan, S. P.; Simpson, S. L.; Thomas, K. V.; Verhagen, R.; Kitajima, M.; Mueller, J. F.; Korajkic, A. Intraday Variability of Indicator and Pathogenic Viruses in 1-h and 24-h Composite Wastewater Samples: Implications for Wastewater-Based Epidemiology. *Environ. Res.* **2021**, *193*, 110531.
- (3) Peccia, J.; Zulli, A.; Brackney, D. E.; Grubaugh, N. D.; Kaplan, E. H.; Casanovas-Massana, A.; Ko, A. I.; Malik, A. A.; Wang, D.; Wang, M.; Warren, J. L.; Weinberger, D. M.; Arnold, W.; Omer, S. B. Measurement of SARS-CoV-2 RNA in Wastewater Tracks Community Infection Dynamics. *Nat. Biotechnol.* **2020**, 38 (10), 1164–1167.
- (4) Lodder, W.; de Roda Husman, A. M. SARS-CoV-2 in Wastewater: Potential Health Risk, but Also Data Source. *Lancet Gastroenterol. Hepatol.* **2020**, *5* (6), 533–534.
- (5) Wu, F.; Xiao, A.; Zhang, J.; Moniz, K.; Endo, N.; Armas, F.; Bonneau, R.; Brown, M. A.; Bushman, M.; Chai, P. R.; Duvallet, C.; Erickson, T. B.; Foppe, K.; Ghaeli, N.; Gu, X.; Hanage, W. P.; Huang, K. H.; Lee, W. L.; Matus, M.; McElroy, K. A.; Nagler, J.; Rhode, S. F.; Santillana, M.; Tucker, J. A.; Wuertz, S.; Zhao, S.; Thompson, J.; Alm, E. J. SARS-CoV-2 Titers in Wastewater Foreshadow Dynamics and Clinical Presentation of New COVID-19 Cases. *medRxiv* 2020, DOI: 10.1101/2020.06.15.20117747.
- (6) Betancourt, W. Q.; Schmitz, B. W.; Innes, G. K.; Prasek, S. M.; Pogreba Brown, K. M.; Stark, E. R.; Foster, A. R.; Sprissler, R. S.; Harris, D. T.; Sherchan, S. P.; Gerba, C. P.; Pepper, I. L. COVID-19 Containment on a College Campus via Wastewater-Based Epidemiology, Targeted Clinical Testing and an Intervention. *Sci. Total Environ.* **2021**, 779, 146408.
- (7) Lu, X.; Wang, L.; Sakthivel, S. K.; Whitaker, B.; Murray, J.; Kamili, S.; Lynch, B.; Malapati, L.; Burke, S. A.; Harcourt, J.; Tamin, A.; Thornburg, N. J.; Villanueva, J. M.; Lindstrom, S. US CDC Real-Time Reverse Transcription PCR Panel for Detection of Severe Acute Respiratory Syndrome Coronavirus 2. *Emerg. Infect. Dis.* **2020**, 26 (8), 1654–1665.
- (8) Bio-Rad SARS-CoV-2 DdPCR Kit: Instructions for Use. 2020.
- (9) Wickham, H. Ggplot2: Elegant Graphics for Data Analysis; Springer-Verlag: New York, 2016.
- (10) Chai, T.; Draxler, R. R. Root Mean Square Error (RMSE) or Mean Absolute Error (MAE)? Arguments against Avoiding RMSE in the Literature. *Geosci. Model Dev.* **2014**, *7* (3), 1247–1250.
- (11) Jeong, J. H.; Woo, J. H.; Park, J. G. Machine Learning Methodology for Management of Shipbuilding Master Data. *Interna-*

tional Journal of Naval Architecture and Ocean Engineering 2020, 12, 428-439.

- (12) Gibas, C.; Lambirth, K.; Mittal, N.; Juel, M. A. I.; Barua, V. B.; Roppolo Brazell, L.; Hinton, K.; Lontai, J.; Stark, N.; Young, I.; Quach, C.; Russ, M.; Kauer, J.; Nicolosi, B.; Chen, D.; Akella, S.; Tang, W.; Schlueter, J.; Munir, M. Implementing Building-Level SARS-CoV-2 Wastewater Surveillance on a University Campus. Sci. Total Environ. 2021, 782, 146749.
- (13) Gerrity, D.; Papp, K.; Stoker, M.; Sims, A.; Frehner, W. Early-Pandemic Wastewater Surveillance of SARS-CoV-2 in Southern Nevada: Methodology, Occurrence, and Incidence/Prevalence Considerations. Water Res. X 2021, 10, 100086.
- (14) Curtis, K.; Keeling, D.; Yetka, K.; Larson, A.; Gonzalez, R. Wastewater SARS-CoV-2 RNA Concentration and Loading Variability from Grab and 24-h Composite Samples. medRxiv 2021, DOI: 10.1101/2020.07.10.20150607.
- (15) Colosi, L. M.; Barry, K. E.; Kotay, S. M.; Porter, M. D.; Poulter, M. D.; Ratliff, C.; Simmons, W.; Steinberg, L. I.; Wilson, D. D.; Morse, R.; Zmick, P.; Mathers, A. J. Development of Wastewater Pooled Surveillance of Severe Acute Respiratory Syndrome Coronavirus 2 (SARS-CoV-2) from Congregate Living Settings. Appl. Environ. Microbiol. 2021, 87 (13), 433-454.

□ Recommended by ACS

Subsewershed SARS-CoV-2 Wastewater Surveillance and COVID-19 Epidemiology Using Building-Specific Occupancy and Case Data

Alasdair Cohen, Peter J. Vikesland, et al.

MAY 13, 2022 ACS FS&T WATER

Relationships between SARS-CoV-2 in Wastewater and COVID-19 Clinical Cases and Hospitalizations, with and without Normalization against Indicators of Huma...

Qingyu Zhan, Helena M. Solo-Gabriele, et al.

MAY 26 2022

ACS ES&T WATER

READ

Pathogen Peak "Averaging" in Potable Reuse Systems: Lessons Learned from Wastewater Surveillance of SARS-CoV-2

Daniel Gerrity, Brian M. Pecson, et al.

JANUARY 12, 2022

ACS ES&T WATER

RFAD 17

Public Awareness of and Support for the Use of Wastewater for SARS-CoV-2 Monitoring: A Community Survey in Louisville, Kentucky

Rochelle H. Holm, Ted Smith, et al.

APRIL 26, 2022

ACS ES&T WATER

READ 2

Get More Suggestions >